Wavelet-ANN Based Detection of Fault Location of Hybrid Renewable Energy Sources Connected Power Transmission System

S. Chandra Shekar*‡ iD , T. Muthamizhan** iD , Mohammad Aijaz*** iD , D.Chandra Sekhar**** iD

*Professor, Department of EEE, NRI Institute of Technology, Agiripalli, Vijayawada Rural, A.P, India.

**Associate Professor, Department of EEE, Sri Sai Ram Institute of Technology, Chennai, India.

***Associate Professor, Department of EEE, Kodada Institute of Technology and Science for Women, Kodad, India.

****Assistant Professor, Department of EEE, Malla Reddy Engineering College, Maisammaguda, Secunderabad, Telangana, India.

(chandrasekharsavarapu@gmail.com, muthamizhan@gmail.com, aijaz.vsce@gmail.com, daram.sekhar@gmail.com)

‡Corresponding Author; S. Chandra Shekar, Professor, Department of EEE, NRI Institute of Technology, Agiripalli, Vijayawada Rural, A.P, India.
Tel: +91 9949294894, chandrasekharsavarapu@gmail.com.

Abstract: The complexity of the power system increases as the hundreds of lines involved due to the penetration of conventional and renewable energy sources to meet the increased load demand. Transmitting the power for hundreds of kilometres long distances makes complexity in the network to locate the fault. Thus it is necessary to develop suitable algorithms to identify the location of the fault accurately in presence of large number of transmission lines. In this paper a novel Wavelet Artificial Neural Network (WANN) based method is developed where the Detailed coefficients (D1 coefficients) obtained from the current signals are used for training and testing ANN. The fault location is carried out in presence of renewable energy sources for various distances, fault impedances on 4-bus connected transmission system. A 4-bus transmission system is simulated using simulation software and the analysis of fault is done by using current signals of various faults with the help of wavelet multi-resolution analysis at both buses. This analysis is worked out almost within half cycle. The proposed wavelet based algorithm is tested for all fault conditions in presence of renewable energy sources with different power ratings at various distances and hence it is proved that the proposed method provided the best results for different fault impedances, fault generator capacities, fault inception angles (FIA).

1. Introduction

The power system is designed to supply continuous power to the end customers without changing voltage, current and frequency levels with minimal cost. But, due to huge penetration of loads to the existing power system, we need to identify the location of disturbances occurring during faults conditions as early as possible and to be cleared using circuit breakers [1]. Here some recent papers are discussed with various techniques for the fault location.

Mahmood Parsia, et al proposes four fault location techniques namely, time-domain, impedance, visual inspection and a novel wavelet-based technique [2]. A new time domain method for fault detection and fault location multi-terminal transmission line wavelet correlated modes is discussed in this paper [3]. The electricity can be produced either directly from photovoltaic cells or indirectly from concentrated solar power technology [4]. Dr. H. V. Gururaja Rao et al a new, simple and dependable wavelet transform based fault location estimator for transmission lines deploying STATCOM

integrating energy storage device [5]. Majid Jamila, Abul Kalama, A.Q. Ansaria, M. Rizwanba presented a novel method of wavelet transform along with a generalized neural network for fault location estimation 2-bus system transmission lines. The fault location accuracy is changing with respect to type fault and the error is more than 2.5% [6]. A. Salehi Dobakhshari and A. M. Ranjbar studied the a Linear Weighted Least-Squares (LWLS) method for fault location on transmission lines by synchronized measurements voltage western systems coordinating council on 9-bus, 22-bus transmission system. The accuracy corresponds to line 18–21 are least with 3% error [7]. Nabamita Roy and Kesab Bhattacharya proposed a method of fault location identification using frequency components of S-Matrices. These components are used as input for the ANN for training the network. A back propagation ANN is used to find fault location. It found the fault location with an error of 4.46% [8]. Alkım Capar, Aysen Basa Arsoy proposed a fault location method using fault voltage and currents vectors on both ends

of transmission line measurements and line parameters. It is found that if the fault is closed at the location of the capacitor the error becomes increasing [9]. Kunjin Chen, Caowei Huang, Jinliang He discussed fault detection techniques using feature extraction from the signal to be analyzed. A D1 review of the methods is discussed for the fault detection, classification and location in transmission and distribution systems. The fault location maximum error was 5% [10]. J. Ren, Member, S. S. Venkata, and E. Sortomme proposed Synchrophasor measurements in distribution systems for the location of the fault in 14-bus distribution feeder. The 1% of change in current and voltage phasor will change the estimated distance value error by 2% [11]. Gaurav Kapoor proposed a scheme for determining the fault location on a 2-bus transmission system using discrete wavelet transform using current signals on both ends of the lines. The fault location error is a maximum of 2.5% [12]. From the above literature survey, few limitations have been observed in fault location. The identification of fault location is dependent on the distance at which the fault occurs in the transmission line. Also, the estimated error of fault location is very high.In this paper a novel WANN based method is developed where the wavelet multi resolution analysis is used to obtain D1 from the fault current signals and this data is used for training and testing ANN. The fault location is carried out in presence of conventional and renewable energy sources on 4-bus connected transmission system. A 4-bus transmission system is simulated using simulation software and the analysis of fault is done by using current signals of various faults. This analysis is worked out almost within half cycle of current signals. The proposed WANN based algorithm is tested for all fault conditions with different power ratings of conventional and renewable energy sources at various distances. Hence it is proved that the proposed method provided the best results for the fault location at different fault impedances, generator capacities, and fault inception angles.

1. Solar Energy

The PV cell equivalent circuit is shown in above Fig.1. The light energy absorbed by the solar cell is represented by its equivalent current source 'I' in parallel with an inverted diode 'D'. It consists of series resistance R_s which represents the resistance due to the diode and metallic contacts and shunt resistance R_{SH} represents the electron-hole recombination. The shunt resistance is having a high value; therefore, it can be neglected [13].
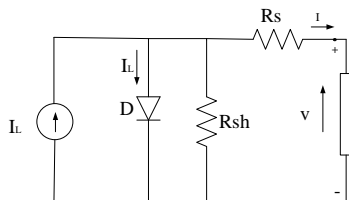

Fig. 1 PV cell equivalent circuit.

An I-V curve starts from a short circuit condition where voltage is minimum and current is at its maximum value and ends at an open circuit condition where the current is zero and voltage are at its maximum value shown in fig.2.. The frequency variation increased is less in case of solar cell

compared to wind energy [14]. At which point cell generates the maximum power is known as MPP Technique. The main criterion to adapt MPP technique is its performance and implementation [15]
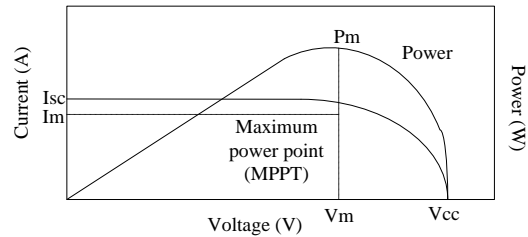

Fig. 2 I-V and P-V Characteristics of solar PV cell

3. Wind Energy

Maximum energy is captured by MPPT algorithm in which maximum mechanical energy is captured by indirect power controller and maximum electrical energy captured by direct power controller [16]. The mechanical power (P_m) extracted from the wind turbine is given as

$$P_m = 1/2 C_P \, \rho V^3_W \, A \, (W)$$

There are two converter controls incorporated in the modelling one is

i) Rotor Side Control Converter (RSCC)

ii) Grid Side Control Converter (GSCC).

The function of RSCC is to extract high amount of power from the wind source and controlling the reactive power inject into the grid. The function of GSCC is to keep DC-bus voltage constant and exchanging reactive power with the grid [17].

4. Technical Challenges in the Integration of Micro Sources

Protection of micro sources connected system poses major technical challenges because of relay operation and coordination in the power system. When the system is operating in both modes of operation, the response of the protection system must be more effective for both internal faults and external faults [18]. During grid-connected mode, if any fault occurs on the MG the desired response is to isolate the micro sources from the MG to protect the loads. The stringent effect of DC off set current makes protection more difficult [19]

5. Wavelets

A wavelet is a small wave, which has finite energy concentrated over a time interval has scaling and shifty properties to suit any type of transient time-frequency varying signals which provides time-frequency localization of a signal having abrupt changes. The mother wavelet is able to the translated and dilated discretely. However, the Wavelet Transform (WT) uses variable window widths (short for high frequencies and longs for low frequencies) and allows in

general obtaining adequate information combining the temporal event with the frequency spectrum [20]. Therefore, it has been selected as an analysis tool. Wavelets are used in the series expansion of functions or signals much similar to the Fourier series [21]. A wave and wavelet is shown in Fig.3.
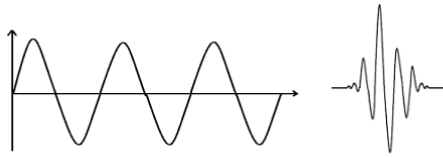

Fig.3. A wave and wavelet

The various types of wavelets are shown in Fig.4. Among these wavelets, the Bior1.5 wavelet is considered because of its unique feature of producing symmetrical coefficients as output from the transient signals [22]
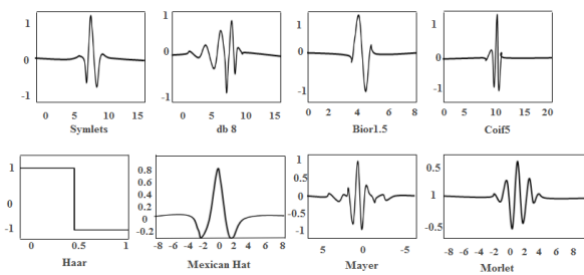

Fig.4. Types of wavelets

6. Artificial Neural Network Structure

ANN's are playing a very crucial role in electrical Power systems applications. Multilayer networks are one among them used for applications of Electrical Power systems. A multilayer neural network consists of more than one layer. Introduction of hidden layers improves the problem solving capability of the network. The general architecture of the Neural Network employed for the proposed fault location algorithm [23] is shown in fig.5.
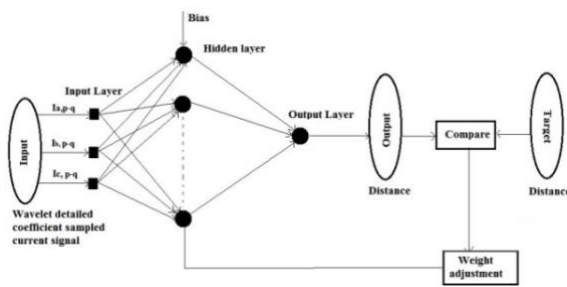

Fig.5. Neural Network Structure.

This network is trained using error back propagation training algorithm. In this training algorithm inputs are presented to the network and outputs of all layers are calculated in the forward direction and error is calculated by comparing the output with the target output and then weights are updated in the backward direction that is weights of output layer are updated first then hidden layer weights based on the error value till the weights of neurons are stabilized. The number of training parameters and training sets is depending on the type of application. The parameter selection plays a vital role

in the stabilization of weights. The main parameters to be selected are

- Initial weights
- Learning coefficient

Weights initiation should be done properly to get the final weights to be stabilized with minimum error. If the initial weights are not selected properly the error may be trapped into local minima or sometimes the weights may not be converged so the training is to be restarted [24]. Similarly, the learning coefficient (usually small) is also to be selected at a small value so that weights will be converged with minimum error. The ANN parameters used for this work are

- ➢ Input data: D1 coefficients of post fault current signals
- ➢ Target data: Line distance
- ➢ Number of layers:2
- ➢ Training algorithm: Back-propagation
- ➢ Number of Patterns: $5 \times 4 \times 4 \times 9 = 720$

(Distances-5, Number of faults-4, Number of buss-4, FIA's-9)

Forward pass
$$H_1 = I_a W_{1a} + I_b W_{1b} + I_c W_{1c} + b_1$$
$$H_2 = I_a W_{2a} + I_b W_{2b} + I_c W_{2c} + b_1$$

$$\vdots \qquad \vdots \qquad \vdots$$

$$H_n = I_a W_{na} + I_b W_{nb} + I_c W_{nc} + b_1$$

Output= $H_1 \times W_1 + H_2 \times W_2 + - - - - - - + H_n \times W_n$
where,
$I_{a,p-q} = $ D1 coefficients of phase-A on p^{th} bus at q^{th} FIA
$I_{b,p-q} = $ D1 coefficients of phase-B on p^{th} bus at q^{th} FIA
$I_{c,p-q} = $ D1 coefficients of phase-C on p^{th} bus at q^{th} FIA

Where,
P = buss (B1, T2, T3, T4)
q = FIAs (0^0, 20^0, 40^0, 60^0, 80^0, 100^0, 120^0, 140^0, 160^0)

$W_{1a}, W_{1b}, W_{1c}, W_{2b}, W_{2b}, W_{3c}, W_{na}, W_{nb}, W_{nc}$ and

$W_1, W_2, - - -W_n$ are initial weights

Activation sigmoid function $= \frac{1}{1+e^{-H_1}}$

Total error $e_t = \sum 1/2(target - output)^2$

Weight update error at $W_n = \frac{\partial e_t}{\partial W_n}$

Location % error $= [\frac{AFL - EFL}{TLL}] \times 100$

AFL is Authentic Fault Location
EFL is Evaluated Fault Location
TLL is Total Line Length.

7. Wavelet-Based Algorithm for the Preparation of Training and Testing Patterns

The proposed wavelet based algorithm is designed for obtaining training and testing patterns of D1 coefficients from the current signals at different distances 10km, 20km, 30km, 40km, 50km for Bus1, Bus2 and 1km, 2km, 3km, 4km, 5km

for Bus3, Bus4 at FIAs 0^0, 20^0, 40^0, 60^0, 80^0, 100^0, 120^0, 140^0, 160^0. After D1 coefficients are obtained, these values given as inputs for ANN and location of fault as target output. Further, the actual distance of fault location is compared with ANN distance. In this paper Bior1.5 wavelet horizontal D1 coefficients of absolute values are used for the analysis.

Designing algorithm

Step-1: Set the bus numbers where the fault is to be analyzed.
Step-2: Apply the fault and measure all the currents of all phases at both ends.
Step-3: Decompose the current signals of each phase by applying the Bior1.5 mother wavelet for all the lines.
Step-4: Obtain the D1 coefficients of current signals.
Step-5: Obtain the absolute value of D1 coefficients.
Step-6: Set the threshold value.
Step-7: Training ANN with D1 coefficients.
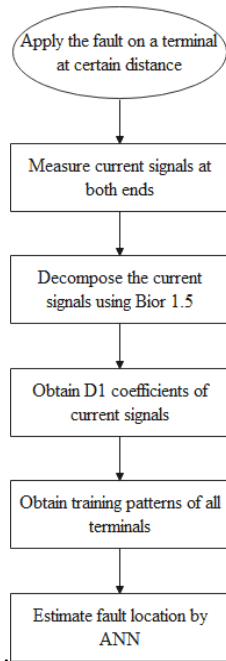
Fig.6. shown flowchart of the proposed algorithm.

Fig.6. Flowchart of Proposed algorithm.

8. Wavelet-ANN Based Technique for Fault Location

A 4-bus renewable energy sources connected transmission system is simulated with 3 different generating capacities show in Table.1.

Table.1. System Data

Bus1	Conventional source	100MVA
Bus2	Utility grid	2500MVA
Bus3	Wind energy source	No.of wind turbines:6, Power rating: 10MW
Bus4	Solar PV source	PV cell Power Rating: 1MW

The proposed 4-bus renewable energy sources connected transmission system is considered for the analysis and shown in fig.7.
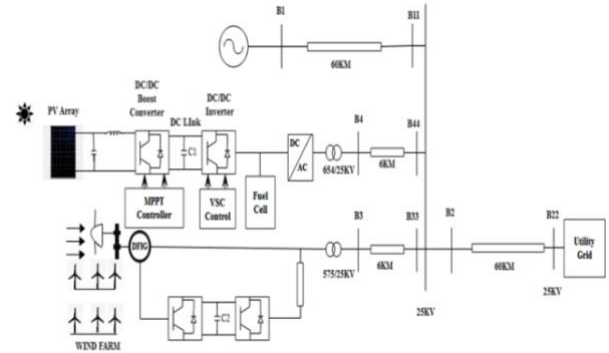
Fig.7. Single line diagram of 4-bus connected transmission system

Line length for Bus1 and Bus2 is 60km line where as for Bus3 and Bus4 is 6km. Symmetrical and unsymmetrical faults are applied to the lines at different distances.

System frequency = 60Hz

Time per cycle $= \frac{1}{60} = 16.6$ (msec)

Sample time $= \frac{1}{60\times36\times100} = \frac{1}{216000}$ (sec)

Total 216000 samples are considered per cycle. Bior1.5 mother wavelet-based algorithm extracts D1 coefficients from current signals. The different types of faults are created at various distances with several fault inception angles in this section. The fault currents are obtained for all these cases and wavelet analysis has been carried out. The D1 coefficients obtained from the wavelet-based algorithm are used for training ANN. After the ANN is trained, it has been tested for different scenarios using the testing data. The testing data contains different faults occurring at several fault inception angles at various distances. The results are presented in section-6.

9. Fault Analysis of 4-bus Renewable Energy Sources Connected Transmission System

The fault analysis with LG, LLG, LL and 3-phase faults on Bus1, Bus2, Bus3 and Bus4 are discussed below.

Training data at B1 with LG (AG) fault

To prepare the necessary training and testing data an LG fault is applied on phase-A at B1 at different distances of 10km, 20km, 30km, 40km, 50km with several FIAs such as 0^0, 20^0, 40^0, 60^0, 80^0, 100^0, 120^0, 140^0, 160^0 and measured the all the phases current signals. The D1 coefficients of all phase currents have been computed as given in Table.2-4. From Table.2-4 it can be observed that the D1 coefficient values corresponding to phase-A have relatively higher compared with phase-B and phase-C. All these D1 coefficient values obtained at various distances and FIA's with different faults are used to train ANN with target value as distance. An example of the training pattern is given below.

Training patterns at B1 with LG (AG) fault

Training patterns are formed with the help of data from Table.2-4.

<u>Example:</u> Consider a distance of 10km and FIA as 0^0. From Table.2-4 take the D1 coefficients corresponding to phase-A, phase-B and phase-C currents. Thus the first training pattern is formed with $I_{a,B1-0} = 1052.7$, $I_{b,B1-0} = 6.03$, $I_{c,B1-0} = 1.681$ as inputs and the distance 10km as target. Similarly, train ANN and corresponding training patterns are given in Table.5. The location error of actual distance and ANN distance using training data and training patterns is given in Table.6. The location absolute error between the AFL and EFL for LG, LLG, 3-phase and LL faults are 1.66 (max.), -1.64 (max.), 1.66 (max.) and 1.33(max.).

Table.2. D1 coefficients of phase-A current at various distances and FIA at B1

FIA/Km	0^0	20^0	40^0	60^0	80^0	100^0	120^0	140^0	160^0
10	1052.7	1061.9	939.32	999.59	1032.8	929.19	892.69	946.96	1065.3
20	773.49	793.01	700.37	764.4	820.98	731.32	697.35	735.75	820.0
30	694.71	692.04	682.22	685.35	732.52	654.65	620.94	648.86	723.7
40	653.38	651.87	667.89	667.68	725.18	656.29	622.11	641.98	712.2
50	628.98	640.54	638.08	720.49	771.52	690.42	656.80	687.57	769.8

Table.3. D1 coefficients of phase-B current at various distances and FIA at B1

FIA/Km	0^0	20^0	40^0	60^0	80^0	100^0	120^0	140^0	160^0
10	6.03	8.362	2.028	9.904	9.468	6.453	7.195	5.838	5.802
20	5.05	7.615	6.021	6.989	5.654	4.490	5.368	5.394	3.726
30	4.12	9.559	3.929	3.454	3.448	3.581	3.613	2.879	2.716
40	2.91	7.016	6.201	5.355	3.804	5.265	5.885	5.654	7.251
50	9.97	1.617	6.013	4.297	3.602	3.780	4.015	2.935	3.094

Table.4. D1 coefficients of phase-C current at various distances and FIA at B1

FIA/Km	0^0	20^0	40^0	60^0	80^0	100^0	120^0	140^0	160^0
10	1.681	2.508	3.869	8.834	8.934	7.790	6.551	5.845	4.639
20	2.458	5.993	3.071	7.671	5.811	6.528	6.296	6.440	5.118
30	7.340	6.536	4.990	3.445	3.254	3.006	3.062	3.326	3.353
40	1.352	2.514	3.504	6.275	3.414	1.844	2.038	2.710	3.732
50	6.374	1.438	2.325	4.782	4.123	3.934	3.336	3.020	3.718

Table.5. Training patterns

Bus(p)-FIA(q)	Ia,p-q	Ib,p-q	Ic,p-q	Target distance
B1-0^0	1052.7	6.03	1.681	
B1-20^0	1061.9	8.362	2.508	
B1-40^0	939.32	2.028	3.869	
B1-60^0	999.59	9.904	8.834	
B1-80^0	1032.8	9.468	8.934	10
B1-100^0	929.19	6.453	7.79	
B1-120^0	892.69	7.195	6.551	
B1-140^0	946.96	5.838	5.845	
B1-160^0	1065.73	5.802	4.639	

B1-0^0	773.49	773.49	2.458	
B1-20^0	793.01	793.01	5.993	
B1-40^0	700.37	700.37	3.071	
B1-60^0	764.4	764.4	7.671	
B1-80^0	820.98	820.98	5.811	20
B1-100^0	731.32	731.32	6.528	
B1-120^0	697.35	697.35	6.296	
B1-140^0	735.75	735.75	6.44	
B1-160^0	820.01	820.01	5.118	
B1-0^0	694.71	4.12	7.34	
B1-20^0	692.04	9.559	6.536	
B1-40^0	682.22	3.929	4.99	
B1-60^0	685.35	3.454	3.445	
B1-80^0	732.52	3.448	3.254	30
B1-100^0	654.65	3.581	3.006	
B1-120^0	620.94	3.613	3.062	
B1-140^0	648.86	2.879	3.326	
B1-160^0	723.75	2.716	3.353	
B1-0^0	653.38	2.91	1.352	
B1-20^0	651.87	7.016	2.514	
B1-40^0	667.89	6.201	3.504	
B1-60^0	667.68	5.355	6.275	
B1-80^0	725.18	3.804	3.414	40
B1-100^0	656.29	5.265	1.844	
B1-120^0	622.11	5.885	2.038	
B1-140^0	641.98	5.654	2.71	
B1-160^0	712.23	7.251	3.732	
B1-0^0	628.98	9.97	6.374	
B1-20^0	640.54	1.617	1.438	
B1-40^0	638.08	6.013	2.325	
B1-60^0	720.49	4.297	4.782	
B1-80^0	771.52	3.602	4.123	50
B1-100^0	690.42	3.78	3.934	
B1-120^0	656.8	4.015	3.336	
B1-140^0	687.57	2.935	3.02	
B1-160^0	769.87	3.094	3.718	

Table.6. Wavelet-ANN based fault location

Actual Distance (km)	ANN Distance (km)		% error	
	B1			
10	LG (AG) fault		LG (AG) fault	
	9.68		0.53	
20	21		-1.66	
30	30.96		-1.6	
40	39.2		1.33	
50	49.7		0.5	
10	LLG (ACG) fault		LLG (ACG) fault	
	9.72	11	0.46	-1.64
20	19.8	19.58	0.2	0.7

30	29.6		30.65		0.66		-1.08
40	39		40.80		1.66		-1.33
50	49		49.76		1.66		0.4
10	**3-phase fault**			**3-phase fault**			
	10.7	11	10.8	-1.3	-1.6	-1.33
20	19.6	19.4	19.2	0.6	1	1.33
30	29.6	31.1	30.2	0.6	-1.8	-0.33
40	40.5	41.8	38.2	-0.9	-0.3	0.93
50	49	49.8	49.1	1.6	0.33	1.5
10	**LL (AB) fault**			**LL (AB) fault**			
	9.68		10.8		0.53		-1.33
20	19.72		19.4		0.46		1
30	29.2		30.8		1.33		-1.33
40	39.3		39.5		1.16		0.833
50	9.68		10.8		0.53		-1.33

Training data at B1 with LLG (ACG) fault

Apply LLG fault on phase-A and phase-C at B1 with different distances 10km, 20km, 30km, 40km, 50km and FIAs 0^0, 20^0, 40^0, 60^0, 80^0, 100^0, 120^0, 140^0, 160^0 and measure current signals as D1 coefficients at all phases as given in Table.7-9.

Table.7. D1 coefficients of phase-A current at various distances and FIA at B1

FIA/Km	0^0	20^0	40^0	60^0	80^0	100^0	120^0	140^0	160^0
10	928.3	984.90	945.00	992.21	1039.4	1163.16	1077.62	987.96	990.44
20	839.7	889.16	782.12	735.74	765.7	854.32	808.05	736.54	731.59
30	678.7	711.05	710.26	586.96	612.0	686.45	651.93	592.55	587.96
40	655.2	692.38	651.09	476.87	512.5	565.15	538.79	479.88	481.89
50	654.0	611.57	624.42	427.97	450.0	505.49	471.74	431.03	429.31

Table.8. D1 coefficients of phase-B current at various distances and FIA at B1

FIA/Km	0^0	20^0	40^0	60^0	80^0	100^0	120^0	140^0	160^0
10	4.284	3.8295	4.2658	6.5004	6.3729	5.0435	6.12	5.77	6.013
20	2.574	2.521	3.2096	9.4736	8.1494	8.3832	7.16	6.32	8.205
30	3.588	2.5518	3.9864	11.6215	8.5848	8.0602	4.74	4.24	6.745
40	8.503	2.5822	9.2304	5.4278	5.2256	3.7492	5.07	5.36	5.647
50	8.534	4.5822	2.2304	8.6158	7.9212	8.1636	7.14	6.39	7.853

Table.9. D1 coefficients of phase-C current at various distances and FIA at B1

FIA/Km	0^0	20^0	40^0	60^0	80^0	100^0	120^0	140^0	160^0
10	955.18	962.59	973.23	1003.76	1110.11	988.25	932.27	961.31	1064.07
20	737.27	816.71	908.54	775.06	861.96	801.14	739.65	745.83	810.09
30	645.08	680.98	755.25	663.87	729.02	710.79	648.93	638.47	680.79
40	634.6	671.56	677.63	622.13	682.49	686.60	630.76	619.39	656.15
50	604.8	603.36	659.42	661.33	720.56	725.43	663.35	647.26	677.39

Table.7-9 it is observed that the D1 coefficient values correspond to phase-A has relatively higher values compared with phase-B and phase-C. All these D1 coefficient values obtained at various distances, various FIA's with different faults are used to train ANN with target value as distance.

Training patterns at B1 with LLG (ACG) fault

Example: Consider a distance of 10km and FIA as 0^0. From the Table.7-9 take the D1 coefficients corresponding to phase-A, phase-B and phase-C. Thus the first training pattern is formed with $I_{a,p-q} = 928.3$, $I_{b,p-q} = 4.2848$, $I_{c,p-q} = 955.18$ as inputs and the distance 10km as target. Similarly, train ANN with all data given in Table.10 gives the fault location.

Table.10. Training patterns for 10km distance

Terminal(p)-FIA(q)	Ia,p-q	Ib,p-q	Ic,p-q	Target distance
B1-0^0	928.3	4.2848	955.18	10
B1-20^0	984.9	3.8295	962.59	
B1-40^0	945	4.2658	973.23	
B1-60^0	992.21	6.5004	1003.76	
B1-80^0	1039.45	6.3729	1110.11	
B1-100^0	1163.16	5.0435	988.25	
B1-120^0	1077.62	6.1257	932.27	
B1-140^0	987.96	5.7767	961.31	
B1-160^0	990.44	6.0138	1064.07	
B1-0^0	839.7	2.5747	737.27	20
B1-20^0	889.16	2.521	816.71	
B1-40^0	782.12	3.2096	908.54	
B1-60^0	735.74	9.4736	775.06	
B1-80^0	765.75	8.1494	861.96	
B1-100^0	854.32	8.3832	801.14	
B1-120^0	808.05	7.1476	739.65	
B1-140^0	736.54	6.3622	745.83	
B1-160^0	731.59	8.2054	810.09	
B1-0^0	678.7	3.5887	645.08	30
B1-20^0	711.05	2.5518	680.98	
B1-40^0	710.26	3.9864	755.25	
B1-60^0	586.96	11.6215	663.87	
B1-80^0	612.7	8.5848	729.02	
B1-100^0	686.45	8.0602	710.79	
B1-120^0	651.93	4.7574	648.93	
B1-140^0	592.55	4.8924	638.47	
B1-160^0	587.96	6.7455	680.79	
B1-0^0	655.2	8.5034	634.6	40
B1-20^0	692.38	2.5822	671.56	
B1-40^0	651.09	9.2304	677.63	
B1-60^0	476.87	5.4278	622.13	
B1-80^0	512.35	5.2256	682.49	
B1-100^0	565.15	3.7492	686.6	
B1-120^0	538.79	5.5207	630.76	
B1-140^0	479.88	5.6636	619.39	
B1-160^0	481.89	5.6477	656.15	
B1-0^0	654	8.5034	604.8	50
B1-20^0	611.57	4.5822	603.36	
B1-40^0	624.42	2.2304	659.42	
B1-60^0	427.97	8.6158	661.33	
B1-80^0	450	7.9212	720.56	
B1-100^0	505.49	8.1636	725.43	
B1-120^0	471.74	7.6314	663.35	
B1-140^0	431.03	6.5339	647.26	
B1-160^0	429.31	7.8531	677.39	

Table.11 is shown the location error of actual distance and ANN distance using the training patterns. The location error between the AFL and EFL is -1.64 (max.).

Table.11. Wavelet-ANN based fault location

Type Fault	Actual Distance (km)	ANN Distance (km)			
		B1		% error	
LLG (BCG)	10	9.72	11	0.46	-1.64
	20	19.88	19.58	0.2	0.7
	30	29.6	30.65	0.66	-1.08
	40	39	40.80	1.66	-1.33
	50	49	49.76	1.66	0.4

Training data at B3 with LLG (BCG) fault

The location error of actual distance and ANN distance using training data and training patterns is given in Table.15 with the help of data from Table.12-14 at B3.

Table.12. D1 Coefficients of Phase-A current at Various Distances and FIA at B3

FIA/Km	0^0	20^0	40^0	60^0	80^0	100^0	120^0	140^0	160^0
10	6.8975	5.4701	7.7936	3.7530	3.9093	3.5245	3.2712	3.4286	5.3056
20	7.7802	9.2221	1.8856	3.6631	3.7689	3.5722	3.7710	3.3902	3.1100
30	3.1311	2.7897	4.0879	3.7910	4.1962	3.9509	5.0422	4.1357	4.3891
40	2.0868	8.7518	3.4168	3.6941	3.5451	3.9366	5.0278	3.7992	4.0208
50	2.4795	5.7869	3.6041	6.3056	6.1226	7.6875	7.7588	7.3832	5.9715

Table.13. D1 Coefficients of Phase-B Current at Various Distances and FIA at B3.

FIA/Km	0^0	20^0	40^0	60^0	80^0	100^0	120^0	140^0	160^0
10	746.85	667.91	684.52	699.91	792.87	707.97	653.26	663.39	732.63
20	683.81	648.82	650.72	568.25	642.54	583.38	535.19	538.80	592.07
30	647.02	664.85	648.97	479.62	542.78	497.08	454.02	454.18	497.44
40	621.77	698.27	631.24	411.16	466.06	429.16	390.93	389.81	426.17
50	615.98	641.93	630.17	354.68	401.91	371.56	337.62	335.65	366.29

Table.14. D1 Coefficiets of Phase-C Current at Various Distances and FIA at B3.

FIA/Km	0^0	20^0	40^0	60^0	80^0	100^0	120^0	140^0	160^0
10	657.74	654.41	684.37	772.21	690.57	640.26	654.75	726.78	739.77
20	636.60	629.81	681.11	617.68	557.15	515.27	525.25	582.15	597.43
30	626.20	623.38	653.09	513.81	462.59	427.88	436.06	483.95	497.03
40	613.07	619.95	645.20	436.78	390.51	362.19	370.57	412.66	421.60
50	603.20	605.60	630.72	372.78	329.83	307.22	316.61	354.04	356.07

Table.15. Wavelet-ANN Based Fault Location

Actual Distance (km)	ANN Distance (km) B3			% error		
1	**LG (AG) fault**			**LG (AG) fault**		
	0.9			1.67		
2	1.92			1.33		
3	2.98			0.33		
4	4.02			-0.33		
5	5.04			-0.66		
1	**LLG (ACG) fault**			**LLG (ACG) fault**		
	0.92	1.02		1.33	-0.33	
2	2.03	1.98		-0.5	0.33	
3	2.98	3.05		0.33	-0.83	
4	3.92	3.90		1.33	1.67	
5	4.96	4.92		0.66	1.33	
1	**3-phase fault**			**3-phase fault**		
	1.02	0.98	1.04	-0.33	0.33	-0.66
2	1.9	2.08	2.04	1.66	-1.33	-0.66
3	2.98	3.02	3.08	0.33	-0.33	-1.33
4	3.98	3.9	4.10	0.33	1.67	-1.67
5	4.96	5.02	5.08	0.66	-0.33	-1.33
1	**LL (AB) fault**			**LL (AB) fault**		
	0.92	1.05		1.33	-0.83	
2	1.90	2.10		1.67	-1.66	
3	2.90	3.04		1.66	-0.66	
4	3.95	4.10		0.83	-1.66	
5	4.90	5.10		1.66	-1.66	

Similarly, training data and training patterns are computed for bus B2, and B4 under different fault conditions. The location error of actual distance and ANN distance using training data and training patterns. The location absolute error between the AFL and EFL for LG, LLG, 3-phase and LL faults are 1.66 (max.), 1.8 (max.), 1.73 (max.) and 1.66 (max.). The D1 coefficients at random distances at B1 is also considered as testing data for the fault location error given in Table.16. Comparison of proposed method with existing method of fault location is given in Table.17.

Table.16. Testing Data

Actual Distance (km)	ANN Distance (km) B1			% error		
12	**LG (AG) fault**			**LG (AG) fault**		
	11.5			0.83		
23	22.3			1.16		
34	33.1			1.5		
45	44.2			1.33		
48	48.5			-0.83		
8	**LLG (ACG) fault**			**LLG (ACG) fault**		
	7.8	8.5		0.33	-0.83	
18	18.5	18.6		-0.83	-1	
32	31.8	32.2		0.33	--0.33	
43	42.5	43.2		0.83	-0.33	
54	53.8	54.6		0.33	-1	
9	**3-phase fault**			**3-phase fault**		
	8.8	9.2	9.8	0.33	-0.33	-1.33
23	22.6	23.4	22.8	0.66	-1	0.33
32	31.2	31.6	31.8	1.33	0.66	0.33

43	42	42.3	42.5	1.66	1.16	0.83
54	53	53.2	53.4	1.66	1.33	1
11	LL (AB) fault			LL (AB) fault		
	9.9	10.5		1.83	-0.83	
21	19.8	20.3		2	1.16	
29	29.1	30.1		-0.16	-0.18	
45	44.2	43.8		1.33	2	
53	52.4	52.09		1	0.151	

Table.17. Comparison of Proposed Method with Existing Method of Fault Location.

S.no	Parameter	Existing method [25]	Proposed method	Observations
1	Wavelet used	Db5 level-5	Bior1.5 level-1	Level-1 is used
2	% error	-1.4 (50km distance) 2.4666 (100km distance)	-0.7333 (50km distance) 0.4666 (100km distance)	Better accuracy

10. Conclusion

From the above analysis we can summarize the conclusions as follows

Fault location analysis of 4-bus renewable energy sources connected transmission system at distances 10km, 20km, 30km, 40km, 50km for conventional and 1km, 2km, 3km, 4km, 5km for Non-conventional sources at various faults and FIAs for various faults has been carried out and compared with existing methods. In this method the current signals are measured at both ends after the fault occurrence and the signals are decomposed by Bior1.5 mother wavelet with wavelet milt-resolution analysis and these decomposed signals further converted into D1 coefficients. These D1 coefficients are in the form of numerical values. These values (higher or lower) depend on magnitude of the fault current signals. After the D1 coefficients are obtained, ANN will be trained with these values. ANN is an ultimate tool for the location of fault using D1 coefficients. Testing data at various random distances like 12km, 23km, 34km, 45km, 48km etc. of 60km line and 1.2km, 2.1km, 3.5km, 4.6km 5.3km etc. with different faults is also developed and tested with ANN. It is found that the fault distance obtained from ANN is very closer to actual distance and the absolute error is maximum of 2% irrespective of fault impedance, fault generator capacities, fault inception angle. So that, the proposed method has shown best results for the detection of fault location of renewable energy sources integrated power transmission system.

References

[1]. Sachit A. Gopalann, Victor Sreeram, Herbert H.C. Iu, "A review of coordination strategies and protection schemes for microgrids", Renewable and Sustainable Energy Reviews 32(2014)222–228.

[2]. Mahmood Parsia , Peter Crossleya, Pier Luigi Dragottib David Cole "Wavelet based fault location on power transmission lines -using real-world travelling wave data" Electric Power Systems Research, Volume 186, September 2020, 106261.

[3].H.Alberto Jimenez, D. Guillen, R. Tapialvera, Gerardo Es cobar, F. Beltran-Carbajal (2021) An improved algorithm for fault detection and location in multi-terminal transmission lines based on wavelet correlation modes. Electric Power Systems Research. 192(3):1-12.

[4]. D. Sakthivadivel, K. Balaji, D. Dsilva Winfred Rufuss, S. Iniyan, L. Suganthi Chapter-1 Solar energy technologies: principles and applications. Renewable Energy Driven Future, 7(6) (2021):3–42.

[5]. Dr. H. V. Gururaja Rao, Dr. Nagesh Prabhu, Dr. R. C. Mala "Wavelet Transform Based fault location estimator for STATCOM compensated lines". Volume 11, Issue 4, June 2020, pp. 309-317.

[6]. Majid Jamila, Abul Kalama, A.Q. Ansaria, M. Rizwanba "Generalized neural network and wavelet transform based approach for fault location estimation of a transmission line" Applied Soft Computing, 19 (2014) 322–332.

[7]. A. Salehi Dobakhshari and A. M. Ranjbar "A Novel Method for Fault Location of Transmission Lines by Wide-Area Voltage Measurements Considering Measurement Errors" IEEE Transactions On Smart Grid, Vol. 6, No. 2, March 2015.

[8]. Nabamita Roy and Kesab Bhattacharya "Detection, Classification, and Estimation of Fault Location on an Overhead Transmission Line Using S-transform and Neural Network", Electric Power Components and Systems, 43(4):461–472, 2015.

[9]. Alkım Capar, Aysen Basa Arsoy "A performance oriented impedance based fault location algorithm for series compensated transmission lines" International Journal of Electrical Power and Energy Systems 71 (2015) 209–214.

[10]. Kunjin Chen, Caowei Huang, Jinliang He "Fault detection, classification and location for transmission lines and distribution systems: a review on the methods" High Voltage., 2016, Vol. 1, Issue. 1, pp. 25–33.

[11]. J. Ren, Member, S. S. Venkata, and E. Sortomme "An Accurate Synchrophasor Based Fault Location Method for Emerging Distribution Systems" IEEE Transactions On Power Delivery, Vol. 29, No. 1, February 2014.

[12]. Gaurav Kapoor "A Discrete Wavelet Transform Approach To Fault Location On A 138kv Two Terminal Transmission Line Using Current Signals Of Both Ends" ISSN: 2395-1680 (ONLINE) ICTACT journal on microelectronics, October 2018, volume: 04, ISSUE: 03.

[13]. Gajendra Singh Chawda, Abdul Gafoor Shaik, Mahmood Shaik, P. Sanjeevikumar, Jens Bo Holm-Nielsen, Om Prakash Mahela, K. Palanisamy, Comprehensive Review on Detection and Classification of Power Quality Disturbances in Utility Grid with Renewable Energy Penetration. IEEE Access. 8(8) (2020):1-25.

[14].Shaowu Li, Aihong Ping, Yefeng Liu, Xiaohong Ma, Chao Li (2020) A variable-weather-parameter MPPT method based on a defined characteristic resistance of photovoltaic cell. Solar Energy. 199(5):673-684.

[15]. H. V. P. Nguyen, T. T. Huynh, V. T. Nguyen 'Comparative Efficiency Assessment of MPPT Algorithms in Photovoltaic Systems' International Journal of Renewable Energy Research, Vol.12, No.4, December 2022: 2061-2067.

[16]. Mostafa Rida, Adel El Samahy, Essam Rashad, Mohamed El Korfolly, Erhab Youssef 'ANN-Based SVC for Optimal Performance of Wind-Driven Self-Excited Synchronous Reluctance Generator' International Journal of Renewable Energy Research, Vol.12, No.4, December 2022: 2082-2091.

[17].Ravi Patel, Faizal Hafiz, Akshya Swain, Abhisek Non linear rotor side converter control of DFIG based wind energy system. Electric Power Systems Research. 198(9) Ukil (2021):1-12.

[18]. Fahad Saleh Al-Ismail DC Microgrid Planning, Operation, and Control: A Comprehensive Review. IEEE Access, 9(3) (2021):36154-36172.

[19]. Ankan Chandra, G K Singh, Vinay Pant (2020) Protection techniques for DC microgrid-A review. Electric Power Systems Research. 187(10) (2021):1-18.

[20]. Sarat Chandra Vegunta, Michael J. Higginson, Yashar E. Kenarangui, George Tsai Li, David W. Zabel, Mohammad Tasdighi, Azadeh Shadman AC Microgrid Protection System Design Challenges—A Practical Experience. Energies. 14(7) (2021):1-23,

[21]. Luis Santiago Azuara Grande,Ricardo Granizo,Santiago Arnaltes [1]Wavelet Analysis to Detect Ground Faults in Electrical Power Systems with Full Penetration of Converter Interface Generation' Electronics 2023, 12(5), 1085.

[22]. K.P. Soman, K.I.Ramachandran, N.G.Resmi "Insight into wavelets from theory to practice" PHI publications, 3rd editon, 2010.

[23] John Abubakar and Ademola Abdulkareem 'Critical Review of Fault Detection, Fault Classification and Fault Location Techniques for Transmission Network' Journal of Engineering Science and Technology Review, 15 (2) (2022) 156 – 166.

[24]. F. B. Costa, A. H. P. Sobrinho, M. Ansaldi, and M. A. D. Almeida, "The effects of the mother wavelet for transmission line fault detection and classification," in Proc. 3rd Int. Youth Conf. Energ. (IYCE), Leiria, Portugal, Jul. 2011, pp. 1–6.

[25] Abdul Gafoor Shaik, Ramana Rao V. Pulipaka 'A new wavelet based fault detection, classification and location in transmission lines' International Journal of Electrical Power and Energy Systems 64 (2015) 35–40.